

# Activation of Slo1 BK channels by Mg<sup>2+</sup> coordinated between the voltage sensor and RCK1 domains

Huanghe Yang, Jingyi Shi, Guohui Zhang, Junqiu Yang, Kelli Delaloye & Jianmin Cui

The voltage-sensor domain (VSD) and the ligand sensor (cytoplasmic domain) of BK channels synergistically control channel activities, thereby integrating electrical and chemical signals for cell function. Studies show that intracellular Mg<sup>2+</sup> mediates the interaction between these sensory domains to activate the channel through an electrostatic interaction with the VSD. Here we report that Mg<sup>2+</sup> binds to a site that consists of amino acid side chains from both the VSD (Asp99 and Asn172) and the cytoplasmic domain (Glu374 and Glu399). For each Mg<sup>2+</sup> binding site, the residues in the VSD and those in the cytoplasmic domain come from neighboring subunits. These results suggest that the VSD and the cytoplasmic domains from different subunits may interact during channel gating, and the packing of VSD or the RCK1 domain to the pore in BK channels differ from that in Kv1.2 or MthK channels.

Many ion channels are assembled from modular elements<sup>1</sup>, in which a sensory module to specific stimuli, such as voltage, ligand binding, post-translational modification and accessory protein association, usually covalently links to the ion-conduction pore and thereby regulates its opening and closing. The direct interaction between the channel pore and various sensory modules in a number of ion channels, such as the membrane-spanning voltage sensor of Kv channels<sup>2</sup>, the cytoplasmic Ca<sup>2+</sup> sensor of MthK channels<sup>3</sup> and the extracellular acetylcholine (ACh) binding domain of ACh receptors<sup>4</sup>, has been proposed as a key step for channel activation. However, how stimuli alter the interaction among different sensors to promote channel activation is still not clear. To address this question, we studied the Slo1 large conductance, voltage- and Ca<sup>2+</sup>-activated K<sup>+</sup> (BK) channel. We chose Slo1 because the BK channel has a distinct VSD and a cytoplasmic ligand binding domain to separately sense membrane voltage and intracellular ligands<sup>5–13</sup>, and previous studies have shown that the two sensory domains interact during channel gating<sup>14</sup>.

BK channels are activated by voltage, intracellular Ca<sup>2+</sup> and Mg<sup>2+</sup> (Fig. 1a,b)<sup>5–7</sup>, and participate in various physiological functions, such as muscle contraction, neural transmission and hearing<sup>7,15–18</sup>. Both sequence homology and experimental evidence suggest that the structure of the VSD in BK channels may resemble that of other Kv channels<sup>19</sup>, whereas the cytoplasmic domain of BK channels may adopt a similar structure to that of the MthK channel<sup>3,8,12,14,20,21</sup>. Previous studies on Mg<sup>2+</sup>-dependent activation of BK channels have revealed structural details that are important for BK channel function. Particularly, two acidic amino acids (Glu374 and Glu399) in the cytoplasmic RCK1 domain of the BK channel may contribute to Mg<sup>2+</sup> coordination<sup>12–14,22</sup>; removal of the side chain carboxylate groups

from these two residues completely abolishes Mg<sup>2+</sup> sensing. These residues in the cytoplasmic domain are located close to the C terminus of the transmembrane segment S4, enabling the bound Mg<sup>2+</sup> to engage in an electrostatic interaction with the voltage-sensing residue Arg213 at the C terminus of S4 (Fig. 1c)<sup>14</sup>.

To further understand the mechanism of Mg<sup>2+</sup>-dependent activation of BK channels and explore the structural basis of the interaction between the VSD and the cytoplasmic domains of mouse Slo1, we studied the composition of the Mg<sup>2+</sup> binding site. As a 'hard' (closed-shell) divalent cation, Mg<sup>2+</sup> is dominantly coordinated by six hard oxygen atoms from the side chains of oxygen-containing residues, main chain carbonyl groups in proteins or water molecules<sup>23</sup> (Fig. 1c, inset). Besides two putative Mg<sup>2+</sup> coordinates contributed by the carboxylate groups from Glu374 and Glu399 (Fig. 1d), four additional oxygen ligands are required for Mg<sup>2+</sup> binding. In this study, we identified two more amino acid side chains, Asp99 and Asn172, in the VSD that may also contribute to Mg<sup>2+</sup> coordination. Notably, our results indicate that Asp99 and Asn172 from the VSD of one subunit may form the Mg<sup>2+</sup> binding site with Glu374 and Glu399 from the cytoplasmic domain of a neighboring subunit. Such an interdomain and intersubunits formation of the Mg<sup>2+</sup> binding site reveals a particular structural alignment of the VSD and the cytoplasmic domain and indicates that the two domains from different subunits may interact during BK channel gating.

## RESULTS

### Alanine scan in the cytoplasmic domain of BK channels

The structure of the cytoplasmic RCK1 domain of MthK (Fig. 1c) has been proposed as the structural model for the cytoplasmic domain of BK channels<sup>3</sup>. The putative Mg<sup>2+</sup> coordinates Glu374 and Glu399 are

Department of Biomedical Engineering, and Cardiac Bioelectricity and Arrhythmia Center, Washington University, 1 Brookings Drive, St. Louis, Missouri 63130, USA. Correspondence should be addressed to J.C. (jcui@biomed.wustl.edu).

Received 13 May; accepted 29 September; published online 19 October 2008; doi:10.1038/nsmb.1507

located at the N terminus of the RCK1 domain (the AC region, colored cyan in Fig. 1c). Because Glu374 and Glu399 are located at the top surface of the cytoplasmic domain, if any side chain from the cytoplasmic domain other than these two residues also contributes to  $Mg^{2+}$  coordination, it should be located in the AC region. To identify such a residue, we carried out alanine scanning of all the residues with oxygen-containing side chains in the AC region. If any of these residues contributes to  $Mg^{2+}$  coordination, the substitution of its side chain with the methyl group of alanine would abolish or substantially reduce the  $Mg^{2+}$ -induced shift of the conductance-voltage ( $G$ - $V$ ) relationship (Fig. 1b). However, except for the mutations of Glu374 and Glu399 (ref. 12), we did not find any alanine mutation that markedly reduced  $Mg^{2+}$  sensing (Fig. 1d, other mutational results have been published previously<sup>12</sup>). Therefore, Glu374 and Glu399 are the only two putative  $Mg^{2+}$  coordinates in the cytoplasmic AC region. Here and in all other figures, the bars represent observed  $G$ - $V$  shifts induced by 10 mM  $[Mg^{2+}]_i$ , subtracting 14.0 mV due to  $Mg^{2+}$  binding to another low-affinity  $Mg^{2+}$  site<sup>24</sup>.

### D99A prevents $Mg^{2+}$ binding

We then examined whether the transmembrane (TM) domain contains side chains that may contribute to  $Mg^{2+}$  coordination. Because mouse Slo1 and *Drosophila melanogaster* SLO channels show similar  $Mg^{2+}$  sensitivity, we mutated 45 oxygen-containing residues in the TM domain that are conserved between these two species and potentially face the cytosol into amino acids that contain no side chain oxygen (Fig. 2a, red and blue). Among these mutations, only D99A, which is located in the C terminus of the S0-S1 linker (Figs. 1c and 2a), completely abolished the  $G$ - $V$  shift induced by 10 mM  $[Mg^{2+}]_i$ ; two other mutations, N172A and Y336A, substantially reduce the  $G$ - $V$  shift (Fig. 2b-d).

Recent studies showed that  $Mg^{2+}$  activates the channel by an electrostatic interaction with Arg213 in S4 after binding to the channel<sup>14</sup>. Therefore, the D99A mutation could eliminate  $Mg^{2+}$  sensitivity by either a direct destruction of the  $Mg^{2+}$  binding site to prevent  $Mg^{2+}$  binding or an alteration of the conformation to prevent the interaction between the bound  $Mg^{2+}$  and Arg213. To distinguish between these two possibilities, we examined whether D99A also abolished the effect of a positive charge covalently added to the vicinity of the  $Mg^{2+}$  binding site. Previous studies showed that Gln397 is located close to the  $Mg^{2+}$  binding site<sup>12,22</sup>. A positive charge covalently added to position 397 by modifying Q397C with 2-(trimethylammonium)ethyl methanethiosulfonate bromide (MTSET(+)) shifts the  $G$ - $V$  relationship to more negative voltages (Fig. 2e). This occurs because the positive charge also interacts with Arg213 electrostatically to activate the channel, mimicking the effects of  $Mg^{2+}$  on the wild-type channel<sup>14</sup>. If D99A alters the conformation of the channel to prevent the interaction between the bound  $Mg^{2+}$  and Arg213, it should also abolish the effects of MTSET(+) modification of Q397C. However, in the presence of D99A, the modification of Cys397 by MTSET(+) still shifted the  $G$ - $V$  relationship by  $-51.7 \pm 1.6$  mV, comparable with the shift in the absence of D99A ( $-66.5 \pm 1.8$  mV) (Fig. 2e). These results indicate that D99A does not substantially alter the electrostatic interaction between the VSD and the positive charge around the  $Mg^{2+}$  binding site.

Next, we measured the effect of D99A on gating currents with and without 10 mM  $[Mg^{2+}]_i$ . The off-gating current ( $I_{gOFF}$ ) is derived from the return of the voltage sensor from the active state to the resting state when most channels are open, whereas the on-gating current ( $I_{gON}$ ) is the result of the movement of the voltage sensor from the resting state to the active state when channels are closed<sup>14,25-27</sup>.

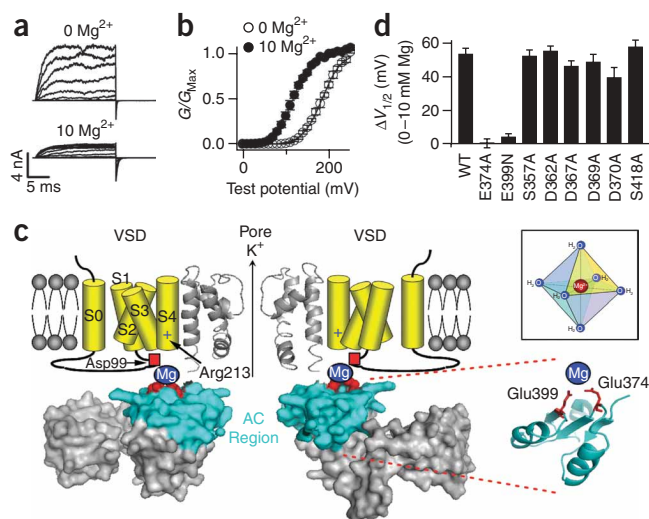


**Figure 1**  $Mg^{2+}$  coordinates in the cytoplasmic domain of the mouse Slo1 channel. (a,b) Representative macroscopic current traces (a) and mean  $G$ - $V$  relationship (b) for wild-type channels in 0 mM and 10 mM  $[Mg^{2+}]_i$ . Testing potentials were from  $-20$  mV to  $240$  mV with  $20$ -mV increments. Both holding and repolarizing potentials were  $-80$  mV. The smooth curves in b represent Boltzmann fits. (c) BK channel model. The pore domain and the cytoplasmic RCK1 domain are based on the MthK crystal structure (PDB 1LNQ)<sup>3</sup>. Transmembrane S0-S4 segments are depicted as cartoons. Only two opposite subunits are shown for clarity. Two putative  $Mg^{2+}$  binding residues (Glu374 and Glu399, red spheres) are located in the AC region (cyan). Inset, the  $Mg^{2+}$  binding site is predominantly formed by six oxygen-containing ligands with an octahedral geometry. (d) Shifts of the  $G$ - $V$  relationship caused by 10 mM  $[Mg^{2+}]_i$  for the alanine mutations of the oxygen-containing residues in the AC region. When the putative  $Mg^{2+}$  binding residues (Glu374 and Glu399) were destroyed, 10 mM  $[Mg^{2+}]_i$  still shifts the  $G$ - $V$  relationship by about  $14$  mV to more negative voltages as a result of  $Mg^{2+}$  binding to a low-affinity  $Mg^{2+}$  site<sup>24</sup>. This effect can be mathematically subtracted to obtain the contribution of the Glu374 and Glu399 site to  $Mg^{2+}$  sensing. Thus, in all figures in this study, the mean  $G$ - $V$  relationships show the observed  $G$ - $V$  shifts induced by 10 mM  $[Mg^{2+}]_i$ , whereas the  $G$ - $V$  shifts in all bar graphs represent the contribution of the Glu374 and Glu399 site after  $14.0$  mV subtraction. Error bars represent s.e.m.

Our recent studies showed that  $Mg^{2+}$  affects wild-type  $I_{gOFF}$  through an electrostatic interaction with Arg213 in S4, primarily when the channel is open<sup>14</sup>. For wild-type channels, 10 mM  $[Mg^{2+}]_i$  reduces the amplitude and the decay rate of the  $I_{gOFF}$  but does not noticeably affect the  $I_{gON}$  (Fig. 2f and Supplementary Fig. 1a online). However, D99A almost abolishes the effect of  $Mg^{2+}$  on  $I_{gOFF}$  (Fig. 2f,g), indicating that S4 can no longer sense  $Mg^{2+}$ . Because D99A does not affect the ability of S4 to sense a positive charge covalently added to the vicinity of the  $Mg^{2+}$  binding site (Fig. 2e), this result indicates that  $Mg^{2+}$  can no longer bind to the site to interact with S4. Similar results were obtained with the mutation E399N, which destroys  $Mg^{2+}$  binding at the Glu374 and Glu399 site (Supplementary Fig. 1). Taken together, mutation D99A destroys  $Mg^{2+}$  binding to the Glu374 and Glu399 site.

### Asp99 is part of the $Mg^{2+}$ binding site

Why does D99A abolish  $Mg^{2+}$  binding? The simplest hypothesis is that the carboxylate group on the side chain of Asp99 provides another  $Mg^{2+}$  coordinate. For this to be true, we should expect (i) that Asp99 is close to residues Glu374 and Glu399 in the cytoplasmic domain so

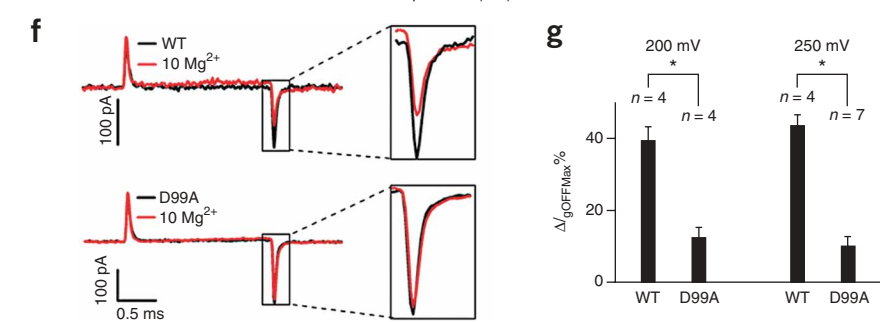
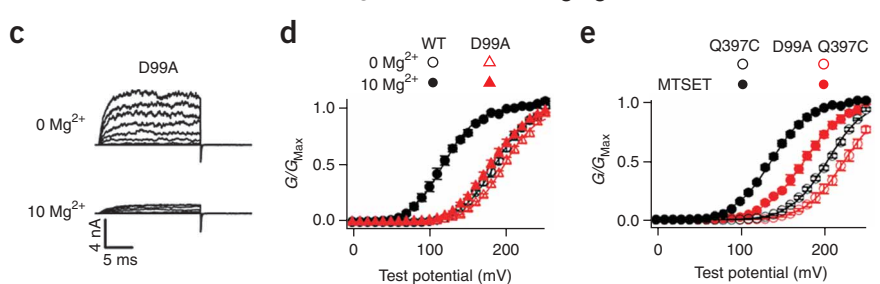
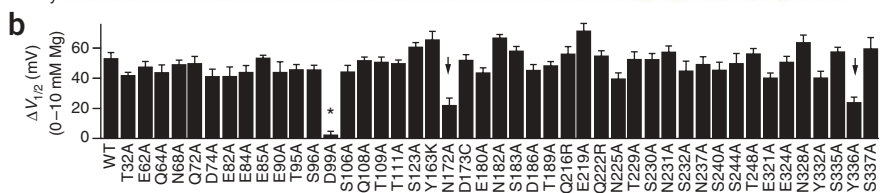
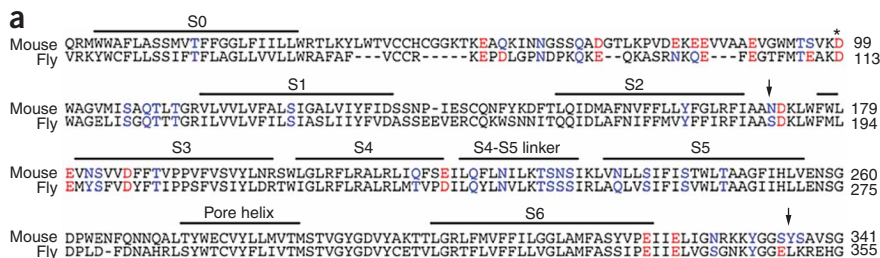


**Figure 2** D99A abolishes  $Mg^{2+}$  sensitivity by preventing  $Mg^{2+}$  binding. **(a)** Sequence alignment of the membrane-spanning (TM) domain in mouse Slo1 and fly SLO channels. Mutations of the oxygen-containing residues that are conserved between mouse Slo1 and fly SLO and potentially face the cytosol (red and blue) were tested. Mouse, Gl 347143; fly (*D. melanogaster*), Gl 115311626. **(b)** Shifts of the  $G$ - $V$  relationship induced by 10 mM  $[Mg^{2+}]_i$  for wild type (WT) and mutant Slo1. **(c)** Macroscopic current traces of D99A in 0 mM and 10 mM  $[Mg^{2+}]_i$ . Testing potentials were from -20 mV to 240 mV with 20-mV increments. Both holding and repolarizing potentials were -80 mV. **(d)**  $G$ - $V$  relationship for wild-type and D99A Slo1. **(e)** Mean  $G$ - $V$  relationship of Q397C and D99A Q397C channels before (open) and after (filled) 200  $\mu$ M MTSET(+) treatment. For all the experiments with MTSET(+) treatment in this study, C430A was used as background to remove the endogenous MTSET effect on channel activation<sup>14,36</sup>. **(f)** Gating current ( $I_g$ ) traces for wild-type (above) and D99A mutant (below) channels with (red) and without (black) 10 mM  $[Mg^{2+}]_i$  in response to a 2-ms, 250-mV depolarizing pulse.  $I_g$  traces of the same patch were first recorded in the absence of  $Mg^{2+}$  and then in 10 mM  $[Mg^{2+}]_i$ . **(g)** Effects of 10 mM  $[Mg^{2+}]_i$  on the reduction of peak OFF-gating currents ( $I_{gOFFMax}$ ) in response to 2-ms, 200-mV or 250-mV depolarizing pulses.

$\Delta I_{gOFFMax}\% = (I_{gOFFMax}(0Mg) - I_{gOFFMax}(10Mg)) / I_{gOFFMax}(0Mg)$ . \* indicates  $P \leq 0.001$ .

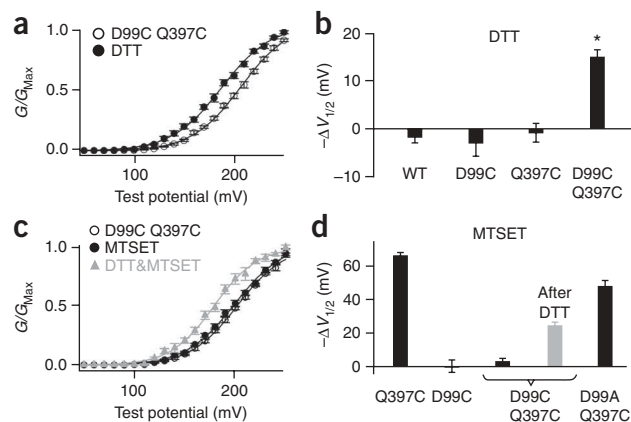
To further demonstrate the existence of this disulfide bond, we treated D99C Q397C mutant channels with 200  $\mu$ M MTSET(+). MTSET(+) treatment of Q397C channels induces a  $-66.5 \pm 1.8$  mV leftward shift of the  $G$ - $V$  relationship in the absence of  $Mg^{2+}$  (Fig. 2e)<sup>14</sup>. A disulfide bond between Cys99 and Cys397 would protect the thiol group on

that they can be part of the same  $Mg^{2+}$  binding site; and (ii) that the oxygen on the side chain of Asp99 is required for  $Mg^{2+}$  binding.

To examine the spatial relationship between Asp99 and the Glu374 and Glu399 site, we made the double mutant D99C Q397C and examined whether a disulfide bond could form between these two cysteine residues. As the  $C_\beta$ - $C_\beta$  distance between two cysteine residues in a disulfide bond is between 2.9 Å to 4.6 Å<sup>28</sup> and Gln397 is close to Glu399 (refs. 12,14,22), a disulfide bond between Cys99 and Cys397 would indicate that Asp99 and Glu374/Glu399 are located within the dimension of a  $Mg^{2+}$  binding site. Treatment of D99C Q397C channels with 10 mM DTT induced a shift of  $-15.0 \pm 1.6$  mV in the  $G$ - $V$  relationship (Fig. 3a,b). This shift is significant compared with the DTT effect on wild-type, D99C and Q397C channels ( $P < 0.001$ ), suggesting a spontaneous disulfide bond formation between Cys99 and Cys397, which is subsequently reduced by DTT.

**Figure 3** Asp99 is spatially close to the cytoplasmic part of the  $Mg^{2+}$  binding site. **(a,b)** Shifts of the  $G$ - $V$  relationship induced by 10 mM DTT in 0 mM  $[Ca^{2+}]_i$  and  $[Mg^{2+}]_i$ . \* indicates  $P < 0.001$ . **(c)** Mean  $G$ - $V$  relationship of D99C Q397C mutant channels before and after 200  $\mu$ M MTSET or sequential DTT-MTSET (gray) treatment in 0 mM  $[Mg^{2+}]_i$ . **(d)**  $G$ - $V$  shifts induced by MTSET treatments, suggesting disulfide formation between Cys99 and Cys397.

residue 397, which would be then no longer available for MTSET(+) to modify, resulting in no MTSET(+) induced  $G$ - $V$  shift. Consistent with this prediction, MTSET(+) did not show any effect on the  $G$ - $V$  relationship of the D99C Q397C channel (Fig. 3c,d). The absence of the MTSET(+) effect is not due to the mutational effect of Asp99, because D99A Q397C channels can still sense MTSET(+), whereas the single mutant D99C is insensitive to MTSET(+) (Figs. 2e and 3d).



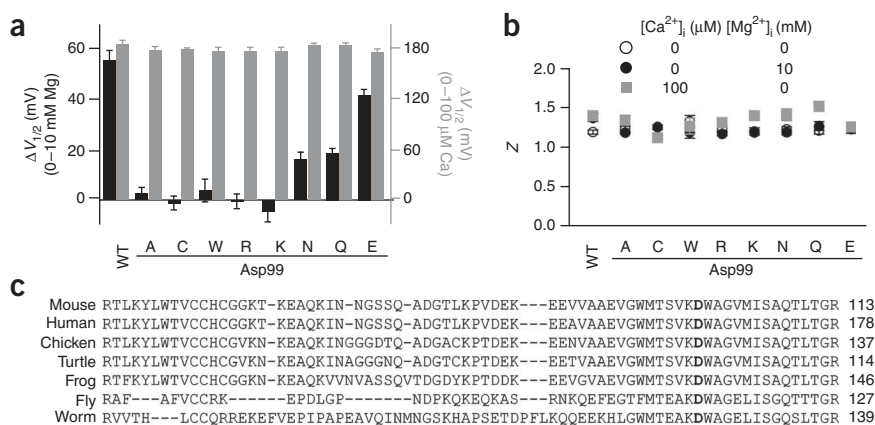


**Figure 4** The side chain carboxylate or carbonyl group of residue 99 is required for  $Mg^{2+}$  coordination. (a)  $G-V$  shifts induced by 10 mM  $[Mg^{2+}]_i$  (black) and by 100  $\mu M$   $[Ca^{2+}]_i$  (gray) for Asp99 mutations. (b) Equivalent gating charge  $z$  of Asp99 mutations. (c) Sequence alignment of the S0-S1 linker from various species: mouse (GI 347143), human (GI 46396283), chicken (GI 46396408), turtle (GI 82224841), frog (GI 46396489), *D. melanogaster* (GI 115311626) and nematode worm (GI 46396994).

The sequential treatment with 10 mM DTT followed by 200  $\mu M$  MTSET(+) resulted in a partial recovery of the MTSET(+) effect ( $-24.5 \pm 2.0$  mV; **Fig. 3c,d**), further indicating the existence of the disulfide bond between Cys99 and Cys397. This partial recovery of the MTSET(+) effect suggests that the disulfide bond between Cys99 and Cys397 is broken by 10 mM DTT in only a fraction of the channels, possibly owing to the rapid reformation of the disulfide bond. Such a phenomenon suggests that Cys99 and Cys397 are located close to each other to allow a fast, spontaneous formation of the disulfide bond. A similar phenomenon has been reported in the study of the cyclic nucleotide-gated channel<sup>29</sup>. Therefore, these experiments indicate that Asp99 in the S0-S1 loop is located spatially close to Gln397, and the Glu374 and Glu399 site, in the cytoplasmic domain.

To test the role of side chain oxygen of residue 99 on  $Mg^{2+}$  sensing, we mutated Asp99 to amino acids with various side chains (**Fig. 4a**).  $Mg^{2+}$  sensing, but not voltage or  $Ca^{2+}$  sensing, is highly correlated with the side chain properties of residue 99 (**Fig. 4a,b**). Similarly to D99A, all the mutations that remove the side chain oxygen (D99C, D99W, D99R and D99K) completely abolished  $Mg^{2+}$  sensitivity, whereas the mutations that preserve the oxygen with carbonyl or carboxylate groups (D99Q, D99N and D99E) retained partial  $Mg^{2+}$  sensitivity. Among these mutations, D99E channels showed higher  $Mg^{2+}$  sensitivity than D99Q and D99N channels. This is consistent with the higher preference of the carboxylate group over the carbonyl group for  $Mg^{2+}$  binding<sup>23</sup>. To the contrary, none of the mutations noticeably altered the  $G-V$  shifts induced by 100  $\mu M$   $[Ca^{2+}]_i$  (**Fig. 4a**) or the equivalent gating charge  $z$  (**Fig. 4b**), indicating that the mutational effect of residue 99 is specific to  $Mg^{2+}$  sensing of the BK channel. Therefore, the oxygen on its side chain is essential for  $Mg^{2+}$  binding. On the basis of the spatial proximity, the mutational effects on  $Mg^{2+}$  sensing and  $Mg^{2+}$  binding, as well as the fact that Asp99 is conserved among BK channels from different species (**Fig. 4c**), we conclude that Asp99 from the VSD and Glu374 and Glu399 from the cytoplasmic domain form a putative interdomain  $Mg^{2+}$  binding site.

### Asn172 also participates in $Mg^{2+}$ binding

In addition to D99A, two other mutations, N172A in the S2-S3 loop and Y336A in the linker connecting S6 to the cytoplasmic domain,

substantially reduced  $Mg^{2+}$  sensing of the channel (**Fig. 2b**). To investigate whether these two residues contribute to  $Mg^{2+}$  coordination, we first mutated them to basic (positively charged) residues (**Fig. 5a,b**). We found that mutating a putative  $Mg^{2+}$  ligand—Glu374, Glu399 (ref. 22) or Asp99 (**Fig. 4a**)—to a basic residue completely abolished  $Mg^{2+}$  sensitivity of the channel due to the destruction of  $Mg^{2+}$  coordination. On the other hand, if a residue (for example, Gln397) is in the vicinity of the  $Mg^{2+}$  binding site but is not a  $Mg^{2+}$  coordinate, positively charged mutations of this residue (that is, Q397R/K) reduced but did not abolish  $Mg^{2+}$  sensitivity, whereas negatively charged mutations (that is, Q397D/E) increased  $Mg^{2+}$  sensitivity<sup>22</sup> (**Fig. 5b**). The change of  $Mg^{2+}$  sensitivity by these mutations might be due to the conformational change of the  $Mg^{2+}$  binding site and/or the electrostatic interactions between  $Mg^{2+}$  and the charges. However, when we tested charged mutations of Tyr336, we

found that both Y336R and Y336E reduced  $Mg^{2+}$  sensitivity, but none of them abolished or enhanced  $Mg^{2+}$  sensitivity (**Fig. 5b**). These phenomena indicate that Tyr336 may not be part of the  $Mg^{2+}$  binding site, nor close enough to the binding site to affect  $Mg^{2+}$  binding through electrostatic interactions. Rather, the reduction of  $Mg^{2+}$  sensitivity is likely to be due to allosteric effects.

In contrast, N172R and N172K completely abolished  $Mg^{2+}$  sensing (**Fig. 5a,b**), whereas N172D and N172E increased  $Mg^{2+}$  sensitivity. Other mutations of Asn172 reduced  $Mg^{2+}$  sensitivity (**Fig. 5a,b**). Does Asn172 contribute to  $Mg^{2+}$  coordination or, alternatively, is it simply close to the  $Mg^{2+}$  binding site such that adding a positive charge on its side chain completely excludes  $Mg^{2+}$  binding, whereas adding a negative charge attracts  $Mg^{2+}$  to bind (**Fig. 5c, inset**)? To answer this question, we tested whether N172D can rescue  $Mg^{2+}$  sensitivity abolished by the mutations of the putative  $Mg^{2+}$  binding residues

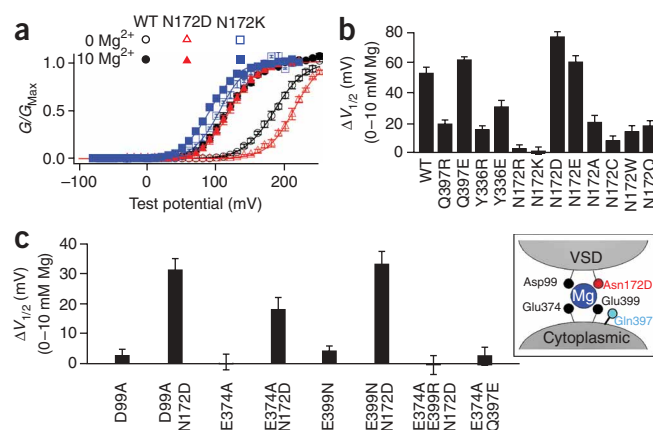


**Figure 5** Asn172 may contribute to  $Mg^{2+}$  coordination. (a) Mean  $G-V$  relationship of wild-type (WT), N172D and N172K mutant channels in 0 mM and 10 mM  $[Mg^{2+}]_i$ . (b) Shifts of the  $G-V$  relationship caused by 10 mM  $[Mg^{2+}]_i$  for the wild type and Gln397, Tyr336 and Asn172 mutations. (c) Shifts of the  $G-V$  relationship caused by 10 mM  $[Mg^{2+}]_i$ . Inset, N172D may substitute other putative  $Mg^{2+}$  coordinates to enable  $Mg^{2+}$  binding.

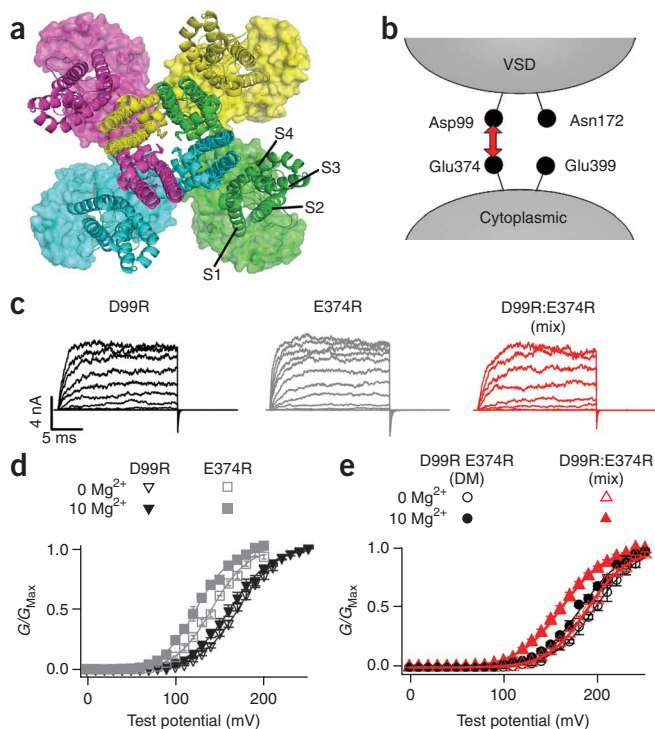


**Figure 6** Asp99 and Glu374 in a  $Mg^{2+}$  binding site are not from the same subunit. **(a)** Superposition of Kv1.2 (ribbons, PDB 2A79)<sup>30</sup> and MthK (surface, PDB 1LNQ)<sup>3</sup> channel structures by aligning their selectivity filter regions. For clarity, the T1 domains of the Kv1.2 structure and the RCK2 domains of the MthK structure are not shown. Different colors represent four subunits. **(b)** Experimental design for mixing D99R and E374R mutations. **(c)** Representative current traces of D99R, E374R and mixed D99R:E374R (1:1) channels. **(d)** Mean  $G$ - $V$  relationship of D99R and E374R channels. The small shift in  $G$ - $V$  relationships is largely due to  $Mg^{2+}$  binding to another low-affinity  $Mg^{2+}$  site<sup>24</sup>. **(e)** Mean  $G$ - $V$  relationship of the D99R E374R double mutant (DM) and D99R:E374R mixed (1:1) channels.

(D99A, E374A or E399N) (Fig. 5c). If Asn172 is part of the  $Mg^{2+}$  binding site, the carboxylate group of N172D may be able to substitute the loss of one carboxylate group induced by single mutations D99A, E374A or E399N, to coordinate  $Mg^{2+}$ . Consistent with this hypothesis, the double-mutant channels containing N172D showed substantially larger  $Mg^{2+}$  sensitivity than these single-mutant channels (Fig. 5c), indicating that N172D can substitute these residues and rescue  $Mg^{2+}$  binding. However, N172D could not rescue any  $Mg^{2+}$  sensitivity from the combinatorial effect of E374A and E399R, which removes two carboxylate groups from the original  $Mg^{2+}$  binding site, suggesting that N172D can compensate for only one lost carboxylate group. Contrary to the effect of N172D, adding a carboxylate group on residue 397 could not rescue any  $Mg^{2+}$  sensitivity when the side chain carboxylate group of Glu374 was removed (Fig. 5c, E374A Q397E). Thus, Asn172 has a different role from Gln397 on  $Mg^{2+}$  binding. These results suggest that the increase of  $Mg^{2+}$  sensitivity by N172D/E or the elimination of the  $Mg^{2+}$  sensitivity by N172R/K cannot be simply attributed to the electrostatic interaction between  $Mg^{2+}$  and the charge on residue 172. Instead, the carboxylate or carbonyl group on the side chain of residue 172 may contribute to  $Mg^{2+}$  coordination.

### $Mg^{2+}$ binding sites are formed between neighboring subunits

It has been proposed that the structures of the VSD and the cytoplasmic RCK1 domain of BK channels resemble that of the VSD of Kv1.2 channels<sup>19</sup> and the RCK domain of MthK channels<sup>3,12,14,22</sup>, respectively. However, it is not clear how these sensory domains align with each other in BK channels. In Figure 6a we combine the structures of Kv1.2 (PDB 2A79)<sup>30</sup> and MthK (PDB 1LNQ)<sup>3</sup> by aligning the selectivity filter of the two channels, which provides an opportunity to examine the packing of different structure domains in the BK channel.

If the VSD and the RCK1 domain of BK channels pack against the pore domain similarly to those of Kv1.2 and MthK, the VSD would be located just above the RCK1 domain from the same subunit (Fig. 6). Such a model would predict that all four  $Mg^{2+}$ -coordinating residues

in each  $Mg^{2+}$  binding site, Asp99, Asn172, Glu374 and Glu399, should come from the same Slo1 protein; that is, the BK channel forms intrasubunit  $Mg^{2+}$  binding sites. To examine this prediction, we mixed single mutations D99R and E374R in a 1:1 ratio (Fig. 6b) and tested their  $Mg^{2+}$  sensitivity (Fig. 6c–e). These mixed single mutants form heterotetrameric channels with various stoichiometry when expressed in *Xenopus laevis* oocytes (Supplementary Fig. 2a online). As each of the single mutations in a  $Mg^{2+}$  binding site is sufficient to abolish  $Mg^{2+}$  binding (Fig. 6c,d), if intrasubunit  $Mg^{2+}$  binding sites are formed, all four sites of a channel should be completely destroyed regardless of the stoichiometry in the heterotetrameric channels (Supplementary Fig. 2a). Therefore, no  $Mg^{2+}$  sensitivity of any mixed channels should be observed. However, when we mixed D99R and E374R in 1:1 ratio, the channels showed a  $-14.8 \pm 1.2$  mV ( $n = 9$ ),  $Mg^{2+}$ -induced  $G$ - $V$  shift (Fig. 6c,e). This residual  $Mg^{2+}$  sensitivity is significantly different ( $P < 0.001$ ) from that of the D99R single mutation ( $n = 13$ ), the E374R single mutation ( $n = 11$ ) or the D99R E374R double mutation ( $n = 7$ ), all of which completely abolished  $Mg^{2+}$  sensing (Fig. 7a).

To explain this phenomenon, we postulated an intersubunit  $Mg^{2+}$  binding site model, in which Asp99 from the VSD and Glu374 from the cytoplasmic domain come from neighboring subunits (Fig. 7b and Supplementary Fig. 2b). According to this model, some D99R:E374R heterotetrameric channels may contain one or two intact  $Mg^{2+}$

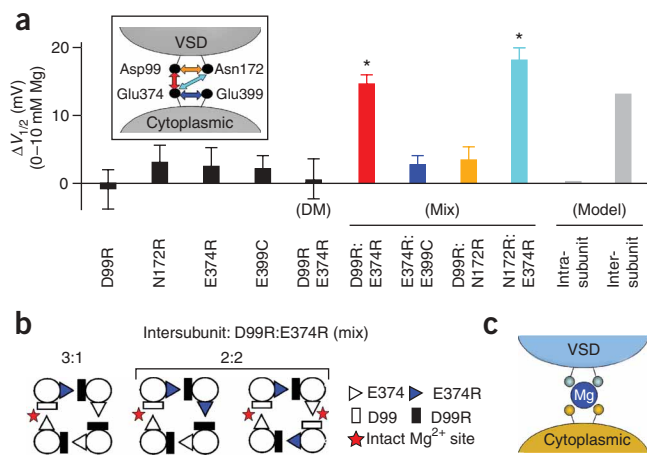


**Figure 7** Asp99 and Asn172, and Glu374 and Glu399, may come from neighboring subunits to form a  $Mg^{2+}$  binding site. **(a)** Shifts of the  $G$ - $V$  relationship caused by 10 mM  $[Mg^{2+}]_i$  for various single and combinations of mutations. Different mixed mutations are color coded as shown by the arrows (inset). All the mixtures have an mRNA ratio of 1:1. Model prediction was calculated based on a binomial distribution (Methods). \* indicates  $P < 0.001$ . **(b)** Intact  $Mg^{2+}$  binding sites can form from mixed mutations based on intersubunit formation of the  $Mg^{2+}$  binding sites. **(c)** Cartoon illustrating interdomain and intersubunit formation of the  $Mg^{2+}$  binding site.

binding site(s). If each binding site is assumed to make an equal contribution to channel activation independently, the model predicts a  $-13.3$  mV shift (25% of that of the wild-type channel) in the  $G$ - $V$  relationship of the mixed channels in the presence of 10 mM  $[\text{Mg}^{2+}]_i$  (Methods and **Supplementary Fig. 2b**). Our experimental observation is consistent with this model prediction (**Fig. 7a**). Current amplitudes of D99R channels, E374R channels and D99R:E374R mixed channels were comparable in these experiments (**Fig. 6c**), indicating that the expression efficiency of D99R and E374R are similar, and hence the mix of D99R and E374R is at a 1:1 ratio.

Similarly, for the 1:1 mixture of N172R:E374R (**Fig. 7a**, inset), 10 mM  $[\text{Mg}^{2+}]_i$  also induced a  $G$ - $V$  shift of  $-18.3 \pm 1.7$  mV (**Fig. 7a**,  $n = 6$ ), suggesting that, in the  $\text{Mg}^{2+}$  binding site, Asn172 and Glu374 also come from neighboring subunits. Contrary to the mix of mutations that are in different domains, the mix of mutations that are in the same domain—that is, D99R:N172R ( $n = 12$ ) in the VSD or E374R:E399C ( $n = 12$ ) in the cytoplasmic domain (**Fig. 7a**, inset)—did not rescue any  $\text{Mg}^{2+}$  sensitivity (**Fig. 7a**). This result rules out the possibility that the rescued  $\text{Mg}^{2+}$  sensitivity is due to some nonspecified artifacts that might have been derived from mixing different mutations. On the basis of all these experiments, we conclude that Asp99 and Asn172 from the VSD and Glu374 and Glu399 from the cytoplasmic domain form an interdomain and intersubunit  $\text{Mg}^{2+}$  binding site (**Fig. 7c**).

## DISCUSSION

Our results show that  $\text{Mg}^{2+}$  is coordinated at the interface between the VSD and the cytoplasmic domain to activate Slo1 BK channels. Side chains from Asp99 and Asn172 in the VSD and Glu374 and Glu399 in the cytoplasmic domain form the putative  $\text{Mg}^{2+}$  binding site. This coordination scheme positions  $\text{Mg}^{2+}$  close to the VSD and enables an electrostatic interaction between the bound  $\text{Mg}^{2+}$  with Arg213 in S4 to affect the movements of the VSD, thereby activating the channel<sup>14</sup>. Notably, the mixture experiments (**Figs. 6** and **7**) suggest that the putative  $\text{Mg}^{2+}$  binding site of BK channels is formed between neighboring subunits. Thus, the VSD and the cytoplasmic domain from different subunits would interact during channel gating.

This special interdomain and intersubunit arrangement of the putative  $\text{Mg}^{2+}$  binding site provides valuable structural and functional information about BK channels. First, the two sensory domains, the VSD and the cytoplasmic domain, are close to each other and may interact intimately during channel gating. According to the octahedral geometry of  $\text{Mg}^{2+}$  binding, the  $\text{Mg}^{2+}$  ligands must be positioned within 5 Å to 6 Å from each other when  $\text{Mg}^{2+}$  binds to the site<sup>23</sup> (**Fig. 1c**, inset). Thus, the top surface of the cytoplasmic domain may make close contact with the intracellular face of the VSD. Our recent study on the electrostatic interaction between Arg213 in S4 and the positive charge on residue 397 suggests that these two positive charges are about 9 Å apart<sup>14</sup>, supporting our current finding on the  $\text{Mg}^{2+}$  binding site and the proximity between these two sensory domains. The disulfide bond between Cys99 and Cys397 (**Fig. 3**) and the ability of N172D to substitute mutations of other  $\text{Mg}^{2+}$  ligands to bind  $\text{Mg}^{2+}$  (**Fig. 5c**) further suggest that these two sensory domains interact closely at their interface. However, it is not clear whether there are other places besides the  $\text{Mg}^{2+}$  binding site where these two sensory domains interact with each other to regulate channel gating. Second, the formation of intersubunit  $\text{Mg}^{2+}$  binding sites suggests that the VSD of one subunit is packed right on top of the cytoplasmic domain from the neighboring subunit (**Fig. 7**). Such a structural arrangement does not agree with the prediction of the quaternary structure model based on the superposition of the Kv1.2 and MthK structures

(**Fig. 6a**). This result indicates that, although the VSD and the cytoplasmic RCK1 domain of BK channels may adopt a similar tertiary structure to that of Kv1.2 and MthK channels<sup>3,8,12,14,19–21</sup>, the packing of the VSD or the cytoplasmic domain relative to the pore domain may differ from that of Kv1.2 or MthK. Such a difference in the quaternary structure may be the result of the unique S0 transmembrane segment<sup>31</sup> and the long S0-S1 loop in the TM domain (**Fig. 2a**) besides the common VSD (S1-S4) that is found in other Kv channels, as well as the intimate interactions between the VSD and the cytoplasmic domain of BK channels. As the packing of the voltage sensor and the cytoplasmic ligand sensor relative to the pore domain may influence the energetic coupling between these sensors and the activation gate, it may contribute to the unique functional properties of the BK channel, such as the allosteric mechanism of voltage- and  $\text{Ca}^{2+}$ -dependent gating<sup>26,32</sup>.

On the basis of a quantum chemistry calculation<sup>23</sup> of the free energy of successive water-exchange reactions in  $\text{Mg}^{2+}$  complexes, Dudev and Lim concluded that neutral carbonyl group(s) (in the case of the mSlo1 BK channel, Asn172) can coordinate  $\text{Mg}^{2+}$  when  $\text{Mg}^{2+}$  is already bound to up to three negatively charged carboxylate groups (Asp99, Glu374 and Glu399 in the mSlo1 BK channel). Under this composition of a  $\text{Mg}^{2+}$  binding site,  $\text{Mg}^{2+}$  cannot exchange all of its first-shell water molecules for protein ligands. In our study, we did not find any residue other than Asp99, Asn172, Glu374 and Glu399 that contributes a potential ligand to  $\text{Mg}^{2+}$  coordination. Our observation is consistent with this theoretical prediction. Therefore, another two coordinates of the  $\text{Mg}^{2+}$  site may come from water molecules. It is also possible that additional water molecule(s) may directly coordinate  $\text{Mg}^{2+}$  such that some of the side chain(s) among Asp99, Asn172, Glu374 and Glu399 may serve as second shell ligand(s) to stabilize these water molecules in the first coordination shell<sup>33</sup>.

According to thermodynamic principles,  $\text{Mg}^{2+}$  binds to the channel with a higher affinity in the open state of the channel than in the closed state, thus facilitating channel opening<sup>24,34,35</sup>. The identification of the interdomain formation of the  $\text{Mg}^{2+}$  binding site in this study provides a possible mechanism to explain the increase of  $\text{Mg}^{2+}$  binding affinity during channel opening. Recent studies on  $\text{Mg}^{2+}$ -dependent activation indicate that the electrostatic interaction between  $\text{Mg}^{2+}$  and the VSD depends on channels opening, suggesting that a relative movement between the cytoplasmic domain and the VSD may occur during channel gating<sup>14,27</sup>. This relative movement may induce rearrangement of the relative orientation of Asp99, Asn172, Glu374 and Glu399, thereby resulting in optimal coordination and higher  $\text{Mg}^{2+}$  binding affinity in the open state.

## METHODS

**Mutagenesis and expression.** We made all channel constructs from the mbr5 clone of the mouse Slo1 BK using PCR with Pfu polymerase (Stratagene). The PCR-amplified regions of all mutants were verified by sequencing. RNA was transcribed *in vitro* with T3 polymerase (Ambion). We injected 0.05–50 ng (for macroscopic currents) or 150–250 ng (for gating currents) of RNA into each *Xenopus laevis* oocyte 2–6 d before recording. For the mixture experiments, the mRNAs of two single mutants were mixed in a 1:1 ratio; the same amount of mRNA of each single mutant was also injected as a control to monitor the expression rate.

**Electrophysiology.** Ionic currents were recorded with inside-out patches using an Axopatch 200-B patch-clamp amplifier (Axon Instruments) and Pulse acquisition software<sup>12</sup> (Heka Elektronik). The pipette solution contained 140 mM potassium methanesulfonic acid, 20 mM HEPES, 2 mM KCl, 2 mM  $\text{MgCl}_2$ , pH 7.2. The basal internal solution contained 140 mM potassium methanesulfonic acid, 20 mM HEPES, 2 mM KCl, pH 7.2.  $\text{MgCl}_2$

was added to the internal solution (with 5 mM EGTA) to give 10 mM free  $[Mg^{2+}]_i$ . A sewer pipe flow system was used to perfuse the internal solution on the cytoplasmic face of the patch.

We recorded gating currents with inside-out patches<sup>25</sup>. The pipette solution contained 127 mM tetraethylammonium (TEA) hydroxide, 125 mM methanesulfonic acid, 2 mM HCl, 2 mM  $MgCl_2$ , 20 mM HEPES, pH 7.2. The internal solution contained 141 mM N-methyl-D-glucamine (NMDG), 135 mM methanesulfonic acid, 6 mM HCl, 20 mM HEPES, 5 mM EGTA, pH 7.2. Gating currents of the same patch were recorded first in the absence of  $Mg^{2+}$ , and then 2.5 M  $MgCl_2$  stock solution was added to the distal place of the bath stage (to avoid the disturbance of the seal of the patch), followed by a 6-min equilibration period to reach the target 10 mM before recording.

Voltage commands were filtered at 20 kHz with an eight-pole Bessel filter (Frequency Devices) to prevent the saturation of fast capacitive transients<sup>25</sup>. Data were sampled at 100 kHz with an 18 bit A/D converter (ITC-18, Instrutech) and filtered at 10 kHz with Axopatch's internal filter. Capacitive transients and leak currents were subtracted using a P/5 protocol with a holding potential of  $-120$  mV. All chemicals were obtained from Sigma-Aldrich unless otherwise noted.

**Chemical modification.** We made 10 mM DTT freshly before each experiment. The inside-out patches were recorded first, followed by a 10-min treatment, and they were then recorded again to measure the DTT effect. MTSET was purchased from Toronto Research Chemicals. An aliquot of 100 mM MTSET stock solution was thawed and diluted 500-fold into the basal internal solution immediately before use. In ionic current recordings, currents were recorded after 2.5 min of MTSET treatment and 0.5 min of washing of the intracellular side of patches.

**Data analysis and the model for the interdomain  $Mg^{2+}$  binding site.** Relative conductance was determined by measuring macroscopic tail current amplitudes at  $-80$  mV. The conductance-voltage ( $G$ - $V$ ) relationships of the wild-type and mutant channels were fitted with the Boltzmann equation (1):

$$G/G_{Max} = 1/(1 + \exp(-ze(V - V_{1/2})/kT)) \quad (1)$$

where  $z$  is the number of equivalent gating charges,  $V_{1/2}$  is the voltage for the channel at half activation,  $e$  is the elementary charge,  $k$  is the Boltzmann's constant and  $T$  is the absolute temperature. Each  $G$ - $V$  curve was obtained from  $n = 5$ –24 patches. Error bars represent s.e.m. in all figures.

**Supplementary Figure 2b** shows all the combinations of D99R:E374R mixture in a 1:1 ratio with a binomial distribution, assuming that the  $Mg^{2+}$  binding site is formed by Asp99 and Glu374 from neighboring subunits. Each BK channel expressed from this mix contains  $n$  subunits of E374R ( $n \leq 4$ ) and  $(4 - n)$  subunits of D99R. Thus, the probability of  $n = 0, 1, 2, 3$  and  $4$  will be 0.0625, 0.25, 0.375, 0.25 and 0.0625, respectively. For  $n = 0$  or  $4$ , the channel is formed by either E374R or D99R so that there is no chance of an intact binding site forming. For  $n = 1$  or  $3$ , there are four different arrangements of the channels, each of which is formed by one E374R and three D99R or vice versa, so that there is always one intact binding site. For  $n = 2$ , there are six different arrangements of the channels, each of which is formed by two E374R and two D99R. Among these six arrangements, four contain one intact binding site and two contain two intact binding sites. Therefore, the probability of forming a channel with 0, 1 and 2 intact binding sites is 0.125, 0.75 and 0.125, respectively. If each intact  $Mg^{2+}$  binding site makes an equal contribution to channel activation independently (25% of total  $Mg^{2+}$  sensing), the remaining  $Mg^{2+}$  sensitivity is given by equation (2):

$$(0.75 \times 0.25 \times 1 + 0.125 \times 0.25 \times 2) \times (-53.2) = 0.25 \times (-53.2) = -13.3 \text{ mV} \quad (2)$$

where  $-53.2$  is the  $Mg^{2+}$  sensitivity contributed by the Glu374 and Glu399 site of the wild-type channels from 0 mM to 10 mM  $[Mg^{2+}]_i$ .

Statistics were performed using SigmaStat 3.5 (Systat Software); a Student's  $t$ -test or one-way ANOVA with an all-pairwise multiple comparison procedure (Tukey test) was performed. A  $P$ -value of  $<0.05$  was considered significant.

**Structural model.** The structure of the  $Mg^{2+}$  binding site of the mouse Slo1 channel was generated based on the crystal structure of the MthK channel by using the PyMol molecular graphics system (<http://www.pymol.org>).

An abstract of this work has been presented in the 52nd Annual Meeting of Biophysical Society.

*Note: Supplementary information is available on the Nature Structural & Molecular Biology website.*

#### ACKNOWLEDGMENTS

We thank L. Hu for calculations of  $Mg^{2+}$  sensitivity according to the model of the intersubunit  $Mg^{2+}$  binding site. We thank C. Lingle, L. Salkoff and L. Hu for critical discussion. The mouse Slo1 clone was provided by L. Salkoff (Washington University). F. Horrigan (Baylor College of Medicine) provided the Y163K mutant mouse Slo1 cDNA. This work was supported by the US National Institutes of Health Grant R01-HL70393 and the National Science Foundation of China Grant 30528011 (J.C.). J.C. is funded by the Spencer T. Olin Endowment.

#### AUTHOR CONTRIBUTIONS

H.Y., J.S. and J.C. designed the research; H.Y., J.S., G.Z., J.Y. and K.D. performed the experiments; H.Y., G.Z. and J.Y. analyzed the data; H.Y. and J.C. wrote the paper.

Published online at <http://www.nature.com/nsmb>

Reprints and permissions information is available online at <http://npg.nature.com/reprintsandpermissions/>

- Hille, B. *Ion Channels Of Excitable Membranes* (Sinauer, Sunderland, MA, 2001).
- Long, S.B., Campbell, E.B. & Mackinnon, R. Voltage sensor of Kv1.2: structural basis of electromechanical coupling. *Science* **309**, 903–908 (2005).
- Jiang, Y. *et al.* Crystal structure and mechanism of a calcium-gated potassium channel. *Nature* **417**, 515–522 (2002).
- Miyazawa, A., Fujiyoshi, Y. & Unwin, N. Structure and gating mechanism of the acetylcholine receptor pore. *Nature* **423**, 949–955 (2003).
- Latorre, R. & Brauchi, S. Large conductance  $Ca^{2+}$ -activated  $K^+$  (BK) channel: activation by  $Ca^{2+}$  and voltage. *Biol. Res.* **39**, 385–401 (2006).
- Magleby, K.L. Gating mechanism of BK (Slo1) channels: so near, yet so far. *J. Gen. Physiol.* **121**, 81–96 (2003).
- Salkoff, L., Butler, A., Ferreira, G., Santi, C. & Wei, A. High-conductance potassium channels of the SLO family. *Nat. Rev. Neurosci.* **7**, 921–931 (2006).
- Hou, S., Xu, R., Heinemann, S.H. & Hoshi, T. Reciprocal regulation of the  $Ca^{2+}$  and  $H^+$  sensitivity in the SLO1 BK channel conferred by the RCK1 domain. *Nat. Struct. Mol. Biol.* **15**, 403–410 (2008).
- Hou, S., Xu, R., Heinemann, S.H. & Hoshi, T. The RCK1 high-affinity  $Ca^{2+}$  sensor confers carbon monoxide sensitivity to Slo1 BK channels. *Proc. Natl. Acad. Sci. USA* **105**, 4039–4043 (2008).
- Tang, X.D. *et al.* Haem can bind to and inhibit mammalian calcium-dependent Slo1 BK channels. *Nature* **425**, 531–535 (2003).
- Zeng, X.H., Xia, X.M. & Lingle, C.J. Divalent cation sensitivity of BK channel activation supports the existence of three distinct binding sites. *J. Gen. Physiol.* **125**, 273–286 (2005).
- Shi, J. *et al.* Mechanism of magnesium activation of calcium-activated potassium channels. *Nature* **418**, 876–880 (2002).
- Xia, X.M., Zeng, X. & Lingle, C.J. Multiple regulatory sites in large-conductance calcium-activated potassium channels. *Nature* **418**, 880–884 (2002).
- Yang, H. *et al.*  $Mg^{2+}$  mediates interaction between the voltage sensor and cytosolic domain to activate BK channels. *Proc. Natl. Acad. Sci. USA* **104**, 18270–18275 (2007).
- Ledoux, J., Werner, M.E., Brayden, J.E. & Nelson, M.T. Calcium-activated potassium channels and the regulation of vascular tone. *Physiology (Bethesda)* **21**, 69–78 (2006).
- Toro, L., Wallner, M., Meera, P. & Tanaka, Y. Maxi- $K_{Ca}$ , a unique member of the voltage-gated K channel superfamily. *News Physiol. Sci.* **13**, 112–117 (1998).
- Fettiplace, R. & Fuchs, P.A. Mechanisms of hair cell tuning. *Annu. Rev. Physiol.* **61**, 809–834 (1999).
- Du, W. *et al.* Calcium-sensitive potassium channelopathy in human epilepsy and paroxysmal movement disorder. *Nat. Genet.* **37**, 733–738 (2005).
- Ma, Z., Lou, X.J. & Horrigan, F.T. Role of charged residues in the S1–S4 voltage sensor of BK channels. *J. Gen. Physiol.* **127**, 309–328 (2006).
- Jiang, Y., Pico, A., Cadene, M., Chait, B.T. & MacKinnon, R. Structure of the RCK domain from the *E. coli*  $K^+$  channel and demonstration of its presence in the human BK channel. *Neuron* **29**, 593–601 (2001).
- Fodor, A.A. & Aldrich, R.W. Statistical limits to the identification of ion channel domains by sequence similarity. *J. Gen. Physiol.* **127**, 755–766 (2006).
- Yang, H., Hu, L., Shi, J. & Cui, J. Tuning magnesium sensitivity of BK channels by mutations. *Biophys. J.* **91**, 2892–2900 (2006).
- Dudev, T. & Lim, C. Principles governing Mg, Ca, and Zn binding and selectivity in proteins. *Chem. Rev.* **103**, 773–788 (2003).

24. Hu, L., Yang, H., Shi, J. & Cui, J. Effects of multiple metal binding sites on calcium and magnesium-dependent activation of BK channels. *J. Gen. Physiol.* **127**, 35–50 (2006).
25. Horrigan, F.T. & Aldrich, R.W. Allosteric voltage gating of potassium channels II. Mslo channel gating charge movement in the absence of  $\text{Ca}^{2+}$ . *J. Gen. Physiol.* **114**, 305–336 (1999).
26. Horrigan, F.T. & Aldrich, R.W. Coupling between voltage sensor activation,  $\text{Ca}^{2+}$  binding and channel opening in large conductance (BK) potassium channels. *J. Gen. Physiol.* **120**, 267–305 (2002).
27. Horrigan, F.T. & Ma, Z.  $\text{Mg}^{2+}$  enhances voltage sensor/gate coupling in BK channels. *J. Gen. Physiol.* **131**, 13–32 (2008).
28. Hazes, B. & Dijkstra, B.W. Model building of disulfide bonds in proteins with known three-dimensional structure. *Protein Eng.* **2**, 119–125 (1988).
29. Flynn, G.E. & Zagotta, W.N. Conformational changes in S6 coupled to the opening of cyclic nucleotide-gated channels. *Neuron* **30**, 689–698 (2001).
30. Long, S.B., Campbell, E.B. & Mackinnon, R. Crystal structure of a mammalian voltage-dependent Shaker family  $\text{K}^+$  channel. *Science* **309**, 897–903 (2005).
31. Wallner, M., Meera, P. & Toro, L. Determinant for  $\beta$ -subunit regulation in high-conductance voltage-activated and  $\text{Ca}^{2+}$ -sensitive  $\text{K}^+$  channels: an additional trans-membrane region at the N terminus. *Proc. Natl. Acad. Sci. USA* **93**, 14922–14927 (1996).
32. Cox, D.H., Cui, J. & Aldrich, R.W. Allosteric gating of a large conductance Ca-activated  $\text{K}^+$  channel. *J. Gen. Physiol.* **110**, 257–281 (1997).
33. Dudev, T., Lin, Y.L., Dudev, M. & Lim, C. First-second shell interactions in metal binding sites in proteins: a PDB survey and DFT/CDM calculations. *J. Am. Chem. Soc.* **125**, 3168–3180 (2003).
34. Shi, J. & Cui, J. Intracellular  $\text{Mg}^{2+}$  enhances the function of BK-type  $\text{Ca}^{2+}$ -activated  $\text{K}^+$  channels. *J. Gen. Physiol.* **118**, 589–606 (2001).
35. Zhang, X., Solaro, C.R. & Lingle, C.J. Allosteric regulation of BK channel gating by  $\text{Ca}^{2+}$  and  $\text{Mg}^{2+}$  through a nonselective, low affinity divalent cation site. *J. Gen. Physiol.* **118**, 607–636 (2001).
36. Zhang, G. & Horrigan, F.T. Cysteine modification alters voltage- and  $\text{Ca}^{2+}$ -dependent gating of large conductance (BK) potassium channels. *J. Gen. Physiol.* **125**, 213–236 (2005).